FIELD THEORY DESIGN OF MILLIMETER-WAVE BANDPASS FILTERS

Jens Bornemann and Ruediger Vahldieck

ABSTRACT

A simplified yet accurate field theory analysis for computer-aided design of millimeter-wave bandpass filters is introduced. By utilizing a TE^{z}_{mn}-mode formulation instead of a generalized approach requiring a superposition of TE_{mn} and TM_{mn} types, the matrix sizes are reduced considerably, resulting in more than 70 percent savings of CPU time. The theoretical results are in excellent agreement with measured data and the software is operational on a personal computer with coprocessor board. Different filter structures are compared to provide the design engineer with better selection criteria.

ZUSAMMENFASSUNG

Es wird eine einheitliche feldtheoretische Analyse zum Entwurf von Millimeterwellen-Bandpassfiltern vorgestellt. Durch die Verwendung einer H^{z}_{mn}-Mode-Formulierung anstatt der Überlagerung von H_{mn}- und E_{mn}-Typen kann die Matrixgrösse wesentlich reduziert und — verglichen mit der vollständigen Modenanalyse im allgemeinen Fall — mehr als 70% an Rechenzeit gespart werden. Mit dem Programm wird nicht nur eine exzellente Übereinstimmung mit gemessenen Daten erreicht, es ist darüber hinaus auf Personal-Computern mit Koprozessor-Einsatz lauffähig. Verschiedene Filterstrukturen werden verglichen, um dem Entwurfs-Ingenieur bessere Auswahlkriterien zur Verfügung zu stellen.

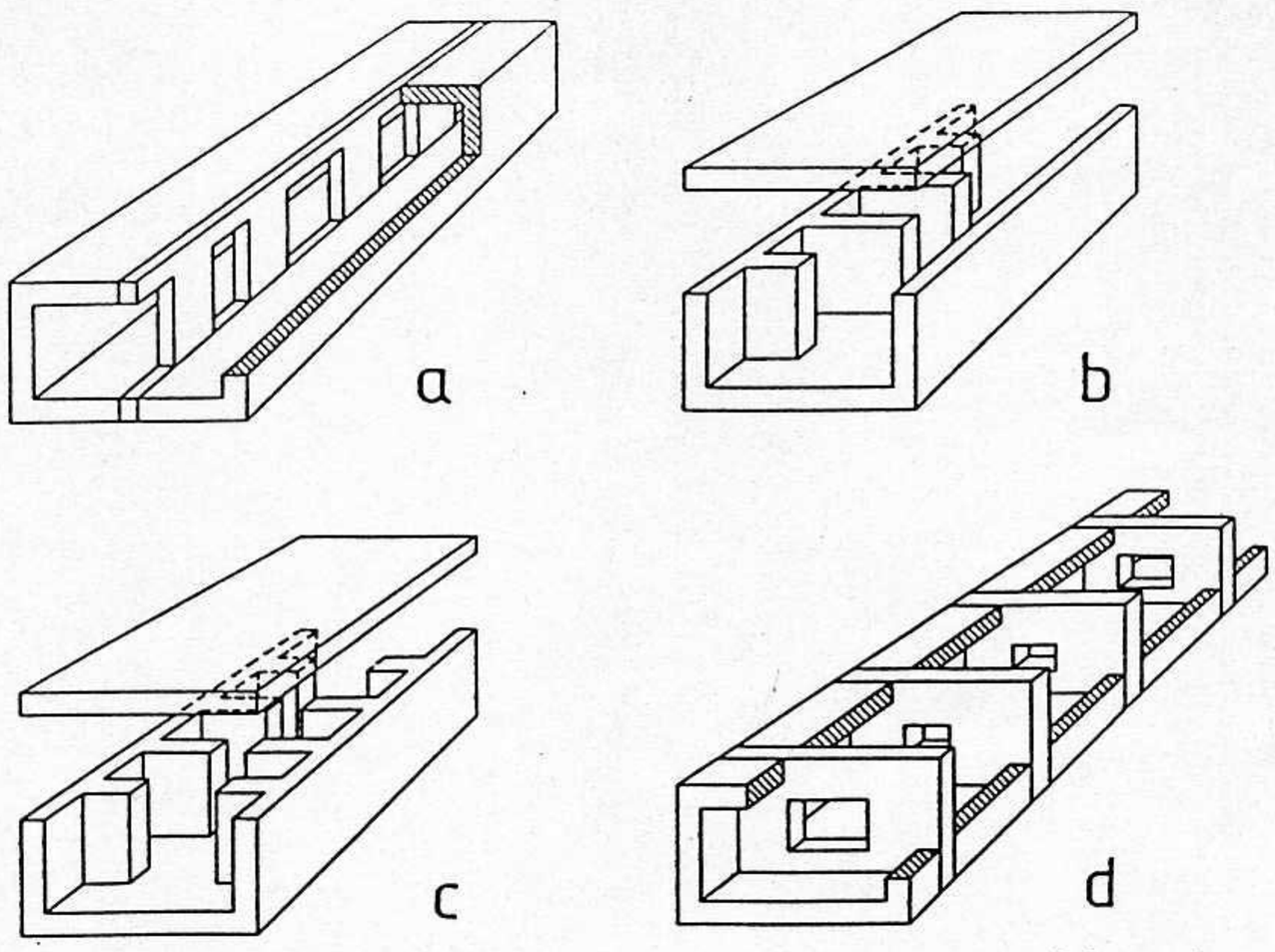

Fig. 1 Millimeter-wave bandpass filters: a) E-plane metal-insert coupled filter; b) single-sided inductive-iris coupled filter; c) double-sided inductive-iris coupled filter; d) resonant-iris coupled filter.

The authors are with the Department of Electrical and Computer Engineering, University of Victoria, P.O. Box 1700, Victoria, B.C., Canada V8W 2Y2, Telephone: (604) 721-8666/8679

INTRODUCTION

Iris-coupled half-wave filters are well-known as compact, high-performance waveguide components in the lower Gigahertz range, e.g. [1-3]. Their application at millimeter-wave frequencies, however, has long been limited by manufacturing tolerances and by the lack of suitable computer-aided design software. The generalized analysis methods presented in [3-5] still require a main-frame computer or at least a powerful work station which generally is not available to the design engineer. The straight-forward filter design [1] does not account for higher-order mode interactions and the finite iris thickness which causes significant deviations particularly at millimeter waves.

Recently, an inductive-iris-coupled waveguide filter (Fig. 1b) operating at 94 GHz has been presented [6]. By using a numerically controlled milling machine tolerances of $\pm 1\mu$m have been achieved. The theoretical filter design procedure, however, is based on the TE_{mo}-mode formulation which is correct only for structures with constant waveguide height.

This paper focuses on a unified field theory analysis of millimeter-wave bandpass filters such as E-plane metal-insert filters (Fig. 1a), single-sided (Fig. 1b) and double-sided (Fig. 1c) inductive-iris coupled filters, and resonant-iris coupled filters (Fig. 1d). The S-matrices of the discontinuities involved can be derived from generalized field equations requiring a superposition of TE_{mn} and TM_{mn} modes or by utilizing a simplified but accurate TE^{x}_{mn}-mode formulation. The latter approach is much more efficient because the matrix sizes are reduced considerably, thus saving more than 70 percent in CPU time compared to the generalized approach. The computer-aided filter design software is operational on a personal computer with coprocessor board, and the results are in excellent agreement with measured data.

THEORY

Resonant-iris coupled filter structures (Fig. 1d) consist of cascaded double-plane waveguide step discontinuities which are characterized by S-parameters usually derived from a linear superposition of TE_{mn} and TM_{mn} modes. The approach requires four field components (E_x, E_y, H_x, H_y) to be matched. As a result, a system involving four matrix equations is obtained, and the resulting matrices to be processed are of size $(N_{TE}+N_{TM})\times(N_{TE}+N_{TM})$. This procedure, although very general, requires main frame computer power and is not suitable for implementation into CAD software on workstation level.

On the other hand the unified TE^{x}_{mn}-mode formulation used in this contribution requires only two field components to satisfy the matching condition, namely E_y and H_x. This is due to the fact that for fundamental-mode operation of the filters, the condition of vanishing E_x-components is incorporated in the field theory treatment and hence need not be part of the matching equations. Therefore, the two relevant field components in iris-coupled half-wave filters can be derived from the x-component of a vector potential $\vec{A}_{hx}$

$$E_y = \frac{\partial A_{hx}}{\partial z}\ , \quad H_x = \frac{j}{\omega\mu}\left[k_o^2 A_{hx} + \frac{\partial^2}{\partial x^2}A_{hx}\right] \tag{1}$$

$$A_{hx} = \sum_{m=0}^{M} \sum_{n=0}^{N} A_{mn} \sin\{k_{xm}(x - x_1)\} \frac{\cos\{k_{yn}(y - y_1)\}}{\sqrt{1 + \delta_{on}}}$$

$$\cdot[V_{mn} \exp(-jk_{zmn}z) - R_{mn} \exp(+jk_{zmn}z)]. \quad (2)$$

For the waveguide-to-iris discontinuity, k_{xm}, k_{yn} and k_{zmn} are the cross-section dependent separation and propagation constants, respectively, A_{mn} is a power normalization term and V_{mn}, R_{mn} are the amplitudes of the waves travelling in $\pm z$-direction; δ_{on} is the Kronecker delta and x_1, y_1 are the x and y offset dimensions for the iris relative to the housing.

By rearranging the order of modes m, n with respect to increasing cutoff frequencies and matching the two field components at the common interface, a matrix size of $N_{TE} \times N_{TE}$ is obtained. This is approximately one quarter of the size used for the conventional TE-TM mode superposition formulation and allows CPU time savings of more than 70 percent in favour of the TE^z_{mn} method described here. (For the further derivation of the modal scattering matrix from the field-matching equations and the procedure to obtain the overall insertion loss behavior of the filter, the reader is referred to [9, 10]).

A variety of filter structures that can be analyzed and designed accurately with this approach is shown in Fig. 1. Although these filters have been treated in the literature before, they are redesigned using the improved algorithm to test its reliability, accuracy, and design time required. The computer-aided design is carried out by using half-wave resonator sections as initial values, and then optimizing [9, 10] the resonator lengths and coupling section (iris, metal insert) dimensions until a specified filter response is obtained. On a personal computer with acceleration board, the CPU time requirements for one set of input parameters vary between 10 seconds for the structure in Fig. 1a and 150 seconds for the structure in Fig. 1d.

RESULTS

Fig. 2 compares the calculated response of a three-resonator resonant-iris coupled filter with experimentally obtained data published in [5]. The excellent agreement between this theory, measurements and the generalized approach presented in [5] verifies the accuracy of the theory given in this paper. Moreover, the CPU time ratio of 3:10 in favor of the TE^z_{mn} procedure proposed here clearly demonstrates its advantage over the method used in [5].

Different filter structures have been designed and compared with respect to their behavior towards higher frequencies in order to provide the design engineer with better selection criteria. Four different three-resonator components have been optimized for a midband frequency of 44 GHz (Q-band) and 1.1 percent bandwidth. Due to the fact that each filter consists of reactance-coupled half-wave resonators, a second passband occurs for the dispersion-reduced harmonic at 75 GHz. Indeed, this resonance may be circumvented by cascading filters with different second passband [2, 7] or by using corrugated waveguide sections [8], but both measures lead to relatively long structures, thus increasing the manufacturing tolerances.

Fig. 3 shows the response of a conventional metal insert filter, e.g. [9]. Since the coupling along the metal insert section increases with frequency, the stopband attenuation starts to decrease at around 54 GHz, which is the cutoff frequency of the coupling sections.

The behavior of a single-sided inductive-iris coupled filter is shown in Fig. 4. Due to the non-symmetrical structure with respect to the waveguide width, the TE_{20} mode (dashed lines) is excited and propagates above 52.7 GHz. This may lead to resonance peaks followed by a steep descent in the attenuation. A similar behavior has been observed in [10] for the TE_{30} mode.

For symmetry reasons, the TE_{20} mode cannot be excited in the double-sided inductive-iris coupled filter (Fig. 5). Since the iris width can be made relatively small, good stopband behavior is obtained up to the second passband at 75 GHz. Improved performance in terms of both, skirt selectivity and stopband attenuation, is provided by the resonant-iris coupled filter as shown in Fig. 6. In terms of electrical performance, which shows passband return losses of better than 20 dB and 60 dB attenuation between 46 and 68 GHz, this design is the most preferable component of the structures investigated. However, in view of its manufacturing, the E-plane filter in Fig. 3 is superior.

CONCLUSION

A unified field theory analysis of millimeter-wave bandpass filters is presented which is based on a TE^{z}_{mn} mode formulation rather than a generalized TE-TM-type description. The fact that only two field components are required for the matching condition instead of four for the TE-TM-type analysis, makes the design software operational on personal computers with accelerator board. Typically CPU time savings of more than 70 percent compared with the TE-TM-type procedure are possible. In view of its electrical performance, the iris-coupled half-wave resonator filter is the most preferable component out of the four investigated.

REFERENCES

[1] Matthaei, G., L. Young, and E.M.T. Jones, *Microwave Filters, Impedance-Matching Networks, and Coupling Structures*, Artech House, 1980, ch. 8, 9.

[2] Chen, T.-S., "Characteristics of waveguide resonant-iris filters", IEEE Trans. Microwave Theory Tech., vol. MTT-15, pp. 260-262, Apr. 1967.

[3] Patzelt, H. and F. Arndt, "Double-plane steps in rectangular waveguides and their application for transformers, irises, and filters", IEEE Trans. Microwave Theory Tech., vol. MTT-30, pp. 771-776, May 1982.

[4] Knetsch, H.D., "Beitrag zur Theorie sprunghafter Querschnittsveränderungen von Hohlleitern", A.E.Ü., Bd. 22, pp. 591-600, Dec. 1968.

[5] Tucholke, U., *Feldtheoretische Analyse und rechnergestützter Entwurf von Resonanzblendenfiltern und Rillenpolarisatoren in Rechteckhohlleitern*, Fortschritt-Berichte VDI, 21/25, VDI-Verlag GmbH, Düsseldorf 1988.

[6] Mahler, W., R. Rathgeber, F. Landstorfer, and W. Holpp, "Rechnergestützter Entwurf von Hohlleiter-Bandpässen in Millimeterwellen-Empfängern", in Proc. MIOP'89 Microwaves and Optronics, 1A3, Feb./Mar. 1989.

[7] Vahldieck, R., "Printed high-power E-plane filters with spurious-free response", in Proc. 16th European Microwave Conf., pp. 281-286, Sep. 1986.

[8] Keller, R., W. Hauth, and U. Rosenberg, "The corrugated waveguide band-pass filter - A new type of waveguide filter", in Proc. MIOP'89 Microwaves and Optronics, P 19, Feb./Mar. 1989.

[9] Vahldieck, R., J. Bornemann, F. Arndt, and D. Grauerholz, "Optimized waveguide E-plane metal insert filters for millimeter-wave applications", IEEE Trans. Microwave Theory Tech., vol. MTT-31, pp. 65-69, Jan. 1963.

[10] Arndt, F., J. Bornemann, D. Heckmann, C. Piontek, H. Semmerow, and H. Schueler, "Modal S-matrix method for the optimum design of inductively direct-coupled cavity filters", IEE Proceedings, vol. 133, Pt. H., pp. 341-350, Oct. 1986.

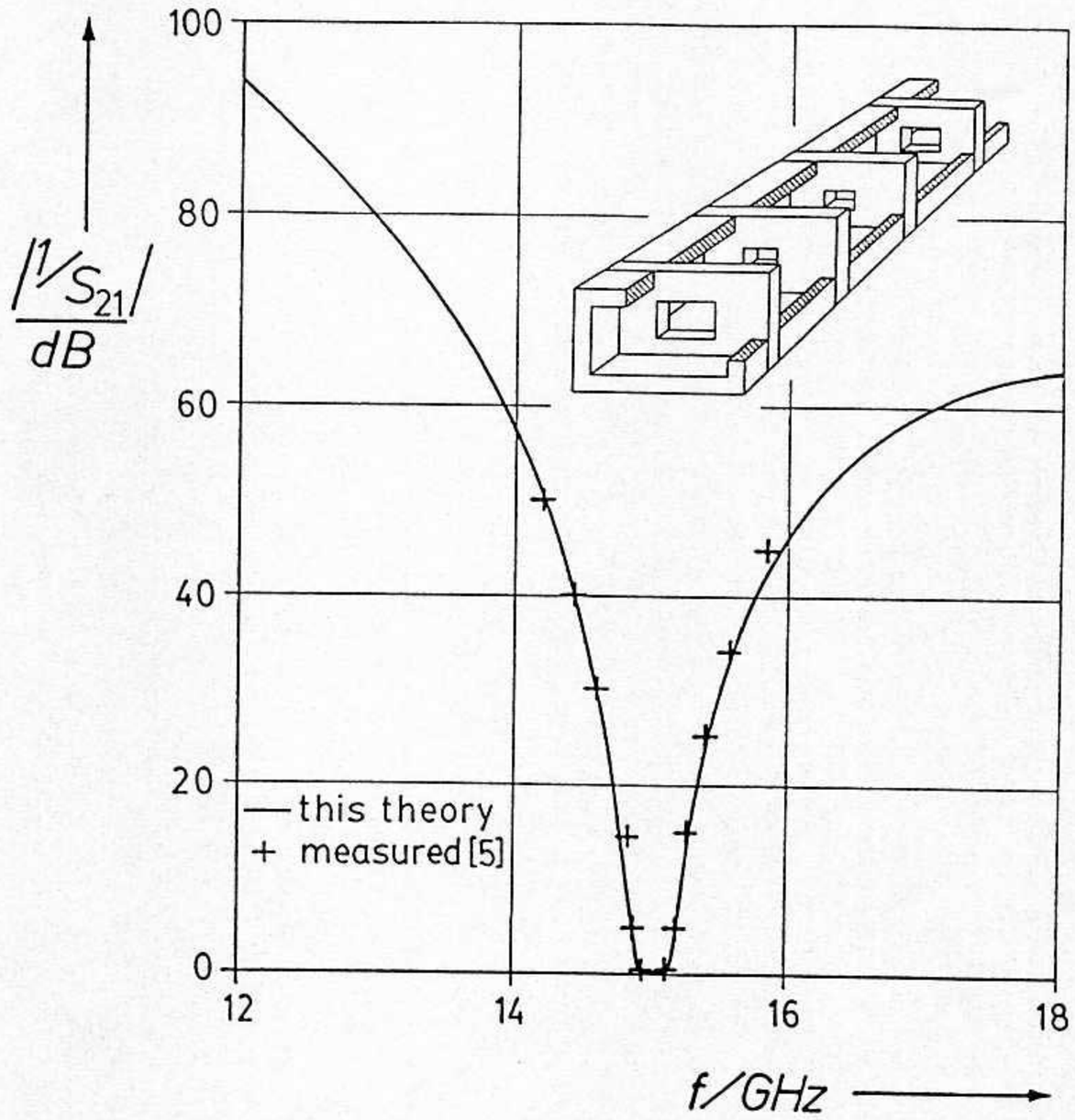

Fig. 2 Calculated response of a three-resonator resonant-iris coupled filter and comparison with measurements [5].

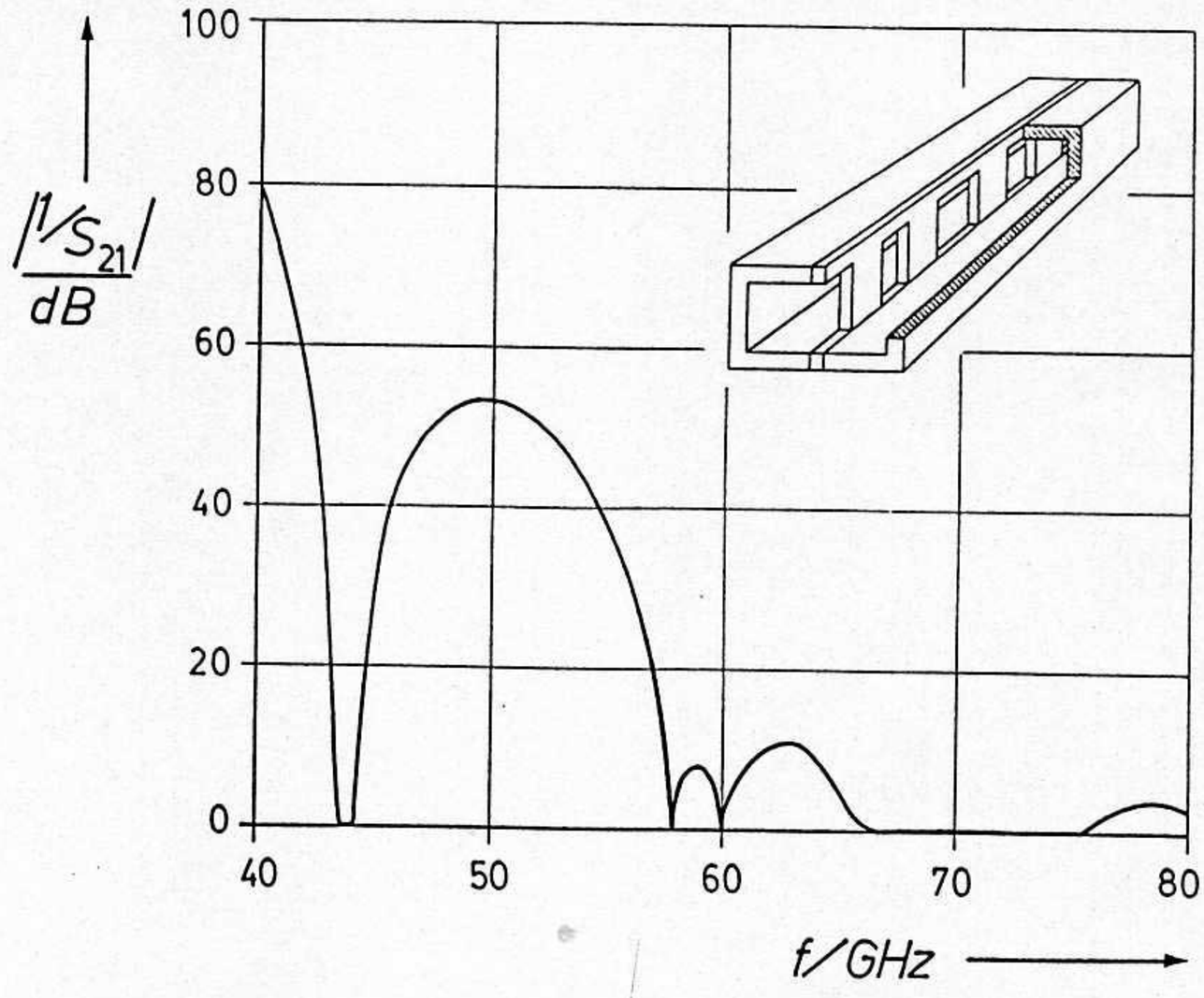

Fig. 3 Response of E-plane metal-insert coupled filter.

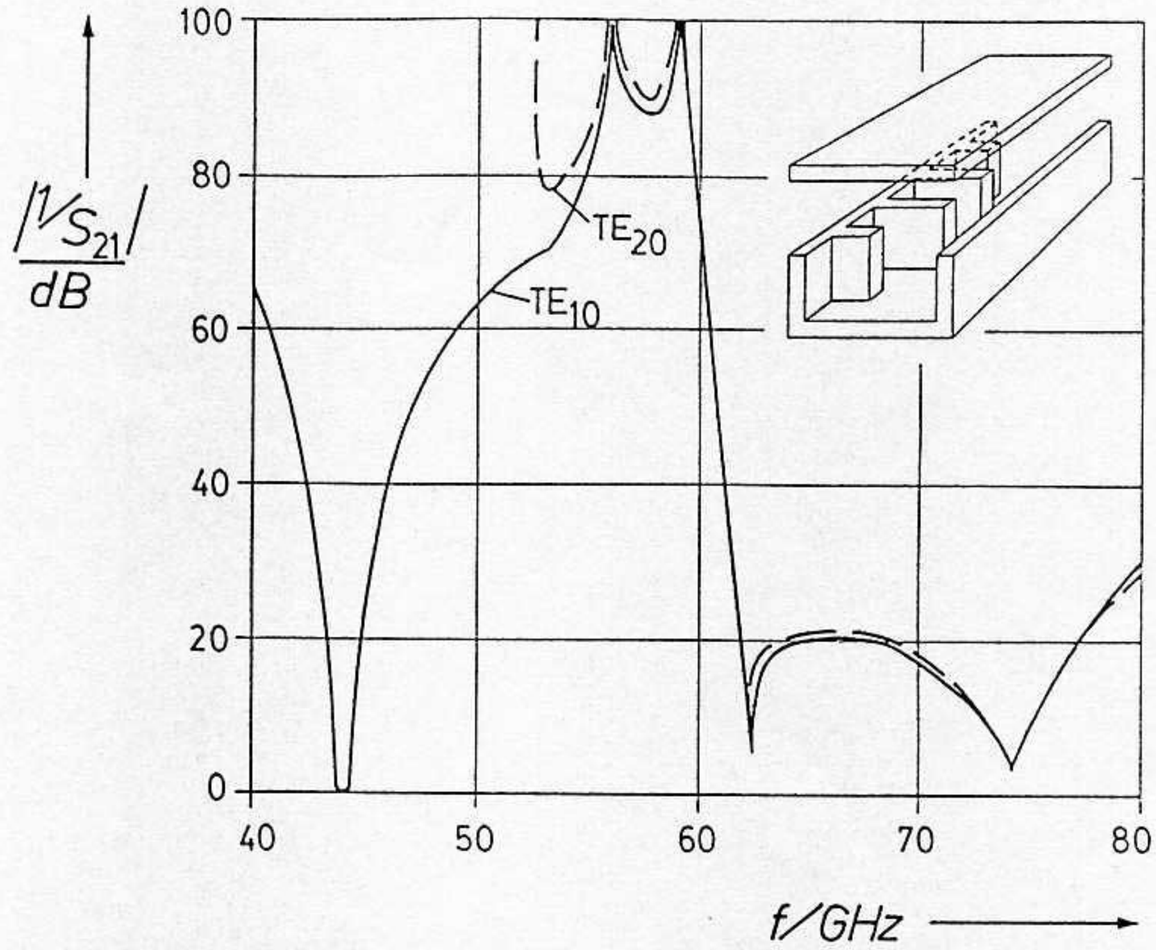

Fig. 4. Response of single-sided inductive-iris coupled filter.

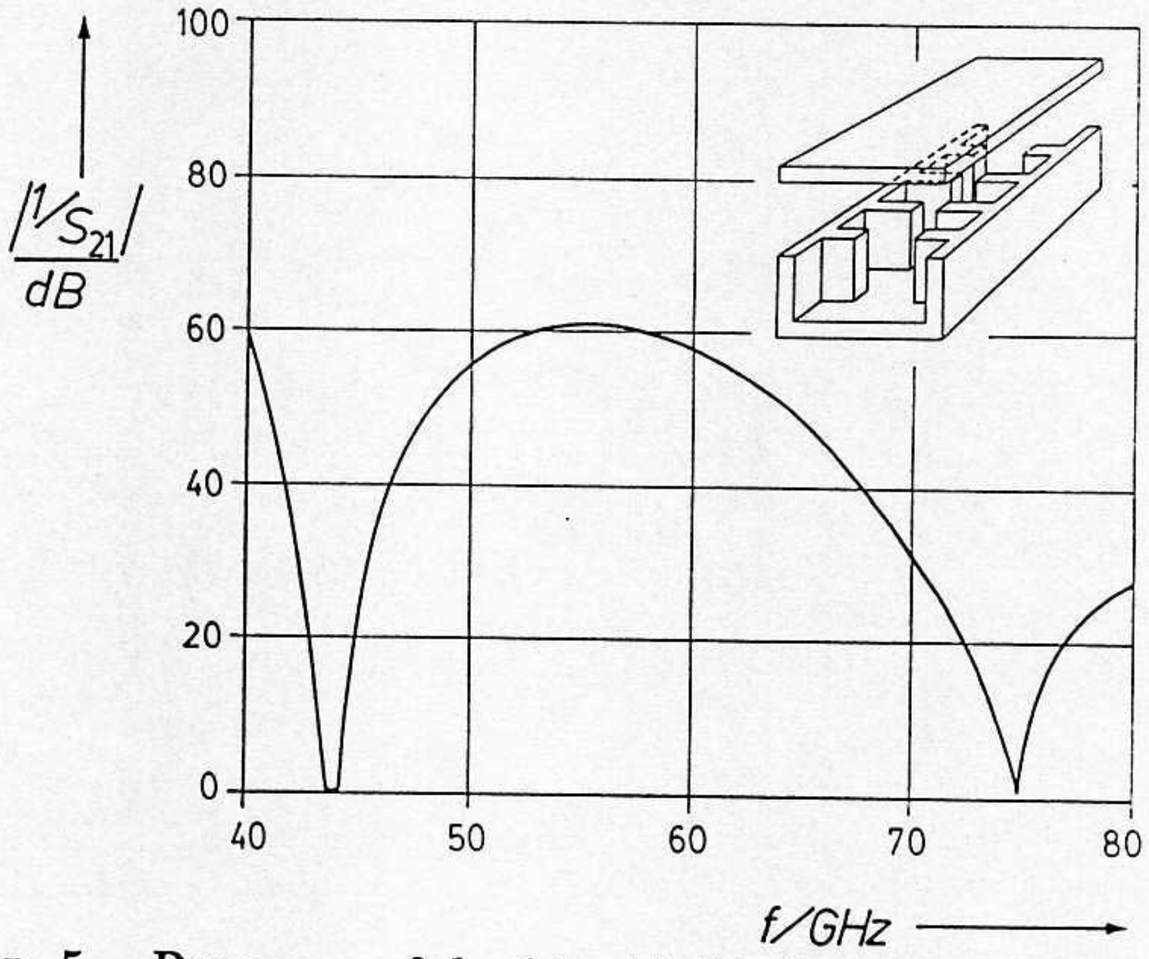

Fig. 5 Response of double-sided inductive-iris coupled filter.

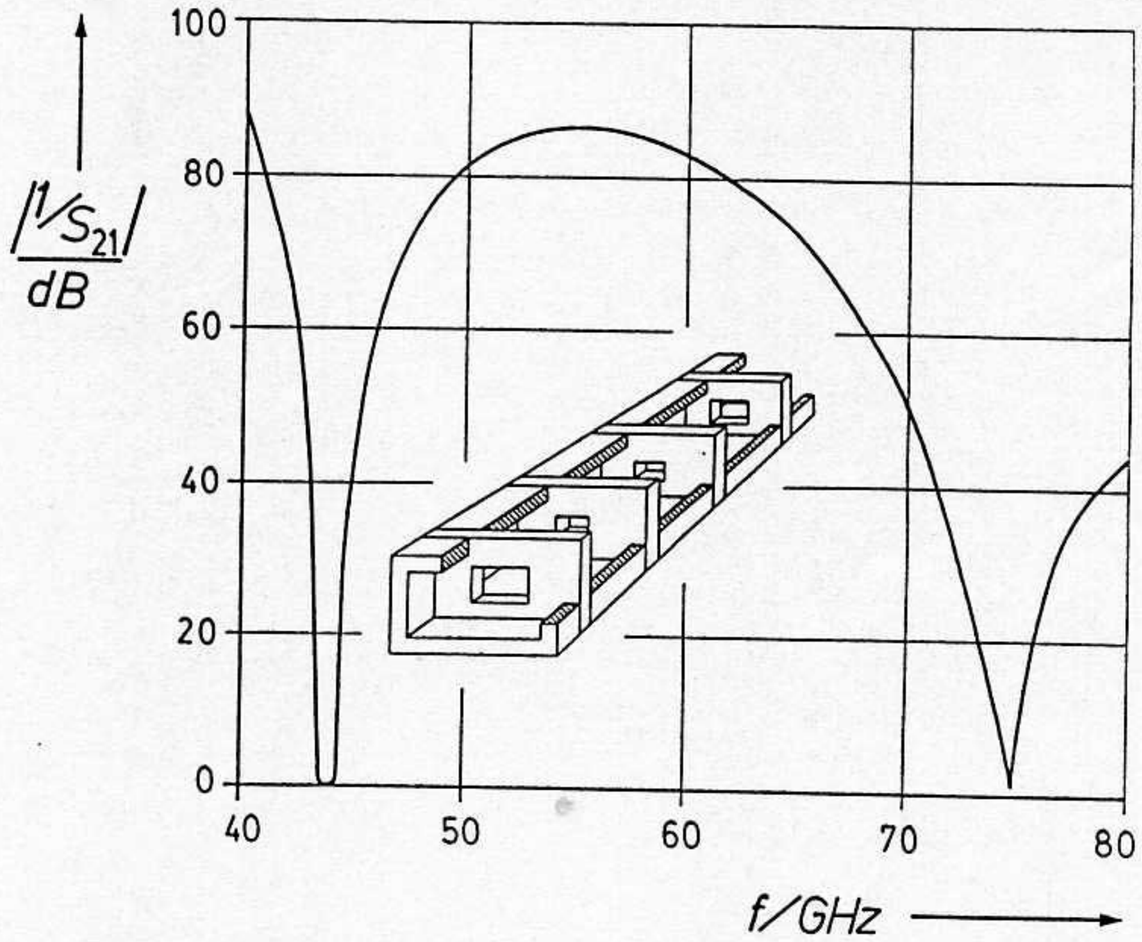

Fig. 6 Response of resonant-iris coupled filter.